Carbohydrate Polymers 117 (2015) 762–770

Contents lists available at ScienceDirect

Carbohydrate Polymers

journal homepage: www.elsevier.com/locate/carbpol

Imino-chitosan biopolymeric films. Obtaining, self-assembling, surface and antimicrobial properties

Luminita Marin[a,*], Daniela Ailincai[a], Mihai Mares[b], Elena Paslaru[a], Mariana Cristea[a], Valentin Nica[c], Bogdan C. Simionescu[a,d]

[a] "Petru Poni" Institute of Macromolecular Chemistry of Romanian Academy, 41A, Aleea Gr. Ghica Voda, Iasi, Romania
[b] "Ion Ionescu de la Brad" University, Laboratory of Antimicrobial Chemotherapy, 8, Aleea Sadoveanu, Iasi, Romania
[c] "Al. I. Cuza" University, Faculty of Physics, 11 Carol I Bulv., Iasi R-700506, Romania
[d] "Gheorghe Asachi" Technical University of Iasi, 73, Bd. Dimitrie Mangeron, Iasi, Romania

ARTICLE INFO

Article history:
Received 6 August 2014
Received in revised form 15 October 2014
Accepted 16 October 2014
Available online 31 October 2014

Paper dedicated to the 65th anniversary of "Petru Poni" Institute of Macromolecular Chemistry of Romanian Academy, Iasi, Romania.

Keywords:
Chitosan
Imine
Film
Trans-imination
Self-assembling
Antimicrobial

ABSTRACT

The paper reports the preparation of twelve imino-chitosan biopolymer films by acid condensation of the amino groups of chitosan with various aldehydes, in aqueous medium, followed by slow water removal. FTIR spectroscopy has shown drastic conformation changes of chitosan macromolecular chains – from a stiff coil to a straight one, while wide angle X-ray diffraction evidenced a layered morphology of the biopolymer films. Contact angle and surface free energy determination indicated a higher biocompatibility of the new biopolymers as compared to the chitosan parent, while the microbiological screening demonstrated their self-defense properties against common and virulent pathogen agents. It was concluded that the reversibility of imine forming promotes the self-assembling of imino-chitosan biopolymer films into a lamellar morphology and, on the other hand, the slow release of the antimicrobial aldehyde in the microbiological culture.

The obtained results demonstrate that chitosan polyamine is a challenging workbench to functional biodynamic materials.

1. Introduction

Prevention of pathogen colonization on food packaging, biological filters, medical implants, medical indwelling devices or ordinary medical devices coming into contact with patients is a major medical and financial matter since infections by microorganisms represent one of the most serious health care complications. To overcome this problem, the development of active antimicrobial materials received considerable attention over the last decades in both building and coating of medical devices (Ferrero, Periolatto, Vineis, & Varesano, 2014; Muzzarelli & Muzzarelli, 2009; Muzzarelli, Tanfani, Emanuelli, & Mariotti, 1982; Nada et al., 2014). In addition, the materials addressed to obtaining of medical implants or medical indwelling devices must be biocompatible, to ensure a good cellular adhesion. Higher cell adhesion and proliferation has been reported for nanostructured films, this demonstrating that morphology is an important feature of the materials coming in direct contact with tissues (Park et al., 2013).

In this context, to meet the long life and easy manufacturing requirements, material formulations include antimicrobial biocompatible polymers. Chitosan is one of the most recommended candidates due to its good biocompatibility, therapeutic properties and lack of toxicity against human body or environment (Croisier & Jérôme, 2013; Muzzarelli, Littarru, Muzzarelli, & Tosi, 2003; Ravi Kumar, Muzzarelli, Muzzarelli, Sashiwa, & Domb, 2004). Besides, the well-known manufacturing of chitosan as films (Saito, Luchnikov, Inaba, & Tamura, 2014), bio-PDLC composites (Marin, Popescu, Zabulica, Uji, & Fron, 2013), micro- and nano-fibers (Yudin et al., 2014), nanoparticles (Sanjai, Kothan, Gonil, Saesoo, & Sajomsang, 2014) or hydrogels (Muzzarelli, 2009; Muzzarelli, Ilari, Xia, Pinotti, & Tomasetti, 1994) further enhances its value, chitosan being of interest for a large number of biomedical, cosmetic, food

* Corresponding author. Tel.: +40 74 9142080.
E-mail address: lmarin@icmpp.ro (L. Marin).

http://dx.doi.org/10.1016/j.carbpol.2014.10.050
0144-8617/

and agricultural applications. On the other hand, while chitosan demonstrated good antimicrobial activity in solution (Guo, Ren, Dong, Wang, & Li, 2013; Kumar, Kumari, Dutta, & Koh, 2014), poor results were reported for chitosan films (Kim et al., 2011). Thus, it was postulated that chitosan antimicrobial activity is given by its ability to bind to the acids found in bacterial membrane, and this is why the contact between chitosan chains and bacteria is imperatively necessary (Raafat, von Bargen, Haas, & Sahl, 2008). In these conditions, one can expect for chitosan films to manifest short time antimicrobial activity followed by the formation of biofilms through bacterial adhesion. To develop antimicrobial chitosan films, various antimicrobial agents as essential oils (Peng & Li, 2014), silver microspheres (An, Ji, Wang, Luo, & Li, 2014) or antimicrobial peptides (Cado et al., 2013) have been encapsulated into the chitosan matrix, providing films with enhanced antimicrobial properties.

Our previous studies revealed that the obtaining of imino-chitosan biopolymers in high yields is possible by condensation of amino groups of chitosan with aldehydes along with slow water removal, when the corresponding films are formed (Marin, Simionescu, & Barboiu, 2012). Condensation of chitosan with proper aldehydes yields films with antimicrobial properties. The reversibility of imine linkage formation plays an important role in films self-organization at nanometric scale, with consequences on their properties, including the gradual release of the antimicrobial aldehyde, i.e. the killing of bacteria on a large area around the biomaterial and preventing biofilm formation (Marin, Stoica et al., 2013).

To accomplish the above mentioned demands in designing biocompatible, antimicrobial materials, twelve biopolymeric films based on chitosan have been prepared. The aldehydes, possessing intrinsic antimicrobial, antifungal, antitumoral a.s.o. biological properties have been chosen with the target to combine the valuable features of the two components and to reach synergistic properties. It is expected that the combination between chitosan and different aldehydes, through a reversible imine bond, will provide an enhanced antimicrobial effect and will induce the ability to acquire films with special morphology, depending on aldehyde structure.

To our knowledge, no literature studies on imino-chitosan films were previously reported.

2. Experimental

2.1. Materials

All reagents were purchased from Aldrich and used without further purification. The molecular weight of chitosan has been calculated to be 263 kDa and its degree of acetylation DA = 15% (Marin et al., 2012, 2014).

2.2. Synthesis

To a 2% solution of chitosan (0.48 g, 2.36 mmol glucosamine repeat units) in 0.7% acetic acid, 2.36 mmol of aldehyde in 3 mL acetone have been slowly added, under vigorous stirring at 60 °C, during 3 h. The reaction was performed into a round flask equipped with a condenser and a magnetic stir bar, for a 1/1 molar ratio of glucosamine/aldehyde groups.

The first visual sign of reaction progress was the color change in beige (citral, cinnamaldehyde) or yellow (vanillin, 2-hydroxi-5nitro-benzaldehyde), or hydrogel obtaining (benzaldehyde, salicylaldehyde, cinnamaldehyde, 2 formylphenyl boronic acid, 2-hydroxy-5-nitro benzaldehyde).

After 3 h reaction time, 3 mL of biopolymer solution was casted into a Petri dish of 3 cm diameter and allowed to slowly dry, at 30 °C. The obtained crude films were further dried in vacuum, at 70 °C, 72 h.

2.3. Investigation methods

Infrared (IR) spectra of dry biopolymer films were recorded on a FT-IR Bruker Vertex 70 Spectrophotometer with a Gemini sampling accessory to collect horizontal attenuated total reflectance (ATR) spectra.

The structural analysis of the pellet samples was performed by powder *wide angle X-ray Diffraction* (WXRD) using an X-ray diffractometer LabXXRD-6000 with CuKα radiation (λ = 0.15406 nm), data being handled by the FullProf 2000 program. Pellet samples were obtained by pressing into a Hydraulic Press, under a pressure of 10 N/m^2.

Film samples were analyzed with a field emission *Scanning Electron Microscope* SEM EDAX – Quanta 200 at an accelerated electron energy of 30 kev.

Atomic force microscopy (AFM) images were collected in semi contact mode with a Solver PRO-M, NT-MDT, Russia instrument. Nova v.1443 software was used for recording and analyzing the AFM topographic and phase contrast images.

Dynamic mechanical analysis was performed in tension mode, on a Perkin Elmer Diamond instrument, on 10 mm × 10 mm film samples of 0.02–0.14 mm thickness. A temperature scan was run with 2 °C/min, at 1 Hz, from −150 °C to 300 °C.

2.3.1. Contact angle measurements and surface free energy calculation

The static contact angle for the film samples was determined by the sessile drop method, at room temperature and controlled humidity, within 10 s, after placing 1 μL drop of water on film surface, using a CAM-200 instrument from KSV Finland. The contact angle was measured by fitting the drop profile using the Young–Laplace equation (Vasile & Pascu, 2007). The contact angle was measured 5 times at different locations on the surface, the average value being considered. To obtain the components of the free surface energy and the total free surface energy, the contact angle at equilibrium between the studied surface and three pure liquids – twice distilled water, formamide and diiodomethane – was measured. The total surface free energy (γ_s^{TOT}) was calculated using the acid base approach of van Oss, Chaudhury, and Good (1988).

2.3.2. Culture media and inoculation

The antimicrobial activity was considered on three different reference strains, i.e. *Escherichia coli* ATCC 25922, *Staphylococcus aureus* ATCC 6583 and *Candida albicans* ATCC 10231.

To assess the antimicrobial activity, the biopolymers were dried under vacuum, at 70 °C for 72 h and stored in a cool dry place until their use. All microorganisms were stored at −80 °C in 10% glycerol. The bacteria were refreshed in Mueller–Hinton broth (Merck) at 36 °C, and afterward were inoculated on Plate Count plates (Biokar, France) for purity checking. Fungi were refreshed on Sabouraud dextrose agar (Biokar, France) and were grown at 36 °C, pH = 7. Microbial suspensions were prepared with these cultures in sterile saline solution to obtain turbidity optically comparable to that of the 0.5 McFarland standards, yielding a suspension containing approximately 1×10^8 CFU mL^{-1} for all microorganisms. Volumes of 0.2 mL from each inoculum were spread onto Mueller–Hinton Agar pre-poured in Petri dishes and the biopolymer films were added after drying of the medium surface. To evaluate the antimicrobial properties, the inhibition of growth was measured under standard conditions after 24 h of incubation at 36 °C. All tests were

carried out in triplicate to verify the results. The diameter of the inhibition zone around the films was measured using a caliper.

3. Results and discussions

Twelve imino-chitosan biopolymers (**CX**) have been obtained by aqueous solution acid condensation of amino groups on chitosan (**C**) chains with different aldehydes (**X**), (Scheme 1). Taking into consideration that reaction equilibrium is moved to the imine formation along with water removing, the reaction mixture was subjected to slow water evaporation to give free standing thin films with high imine linkages content (Marin et al., 2012; Sagiomo & Luning, 2009).

The formation of imine bonds in imino-chitosan biopolymeric films was proved by solid state ^{13}C NMR spectroscopy, which revealed the appearance of the chemical shift characteristic to the imine carbon around 165 ppm (Fig. 1s).

FTIR spectra of biopolymer films show a significant shape change as compared to chitosan, indicating imine bond formation and supramolecular structure modifications. Imine bond formation is confirmed by a sharp, intense absorption band in the 1630–1640 cm^{-1} range, characteristic to the group stretching vibrations of the CH=N linkage (Caro et al., 2013; Guinesi & Cavalheiro, 2006). At the same time, the band around 1543 cm^{-1} characteristic to free amino groups at C2 position of glucosamine shifted to higher wavenumber and decreased in intensity, suggesting the consuming of the chitosan amino functional groups along with imine linkage formation. The absorption band specific to the functional aldehyde group disappeared, whilst the other bands specific to aldehyde residue within imine unit were present, indicating the complete condensation of aldehyde reagents. Compared to the aromatic imine FTIR spectra (Marin, Harabagiu, van der Lee, Arvinte, & Barboiu, 2013), the position of CH=N stretching band in the studied biopolymers is shifted toward higher wavenumbers, reflecting the aliphatic nature of chitosan which led to a shorter conjugation length. Therefore, the imine band (1625–1640 cm^{-1}) lays quite close to characteristic amide I in chitosan band (around 1650 cm^{-1}) (Brugnerotto et al., 2001), in some cases superposing each other, and hence their difficult attribution. Fig. 1a gives the finger print region of chitosan and two representative biopolymer FTIR spectra as an example.

Important changes of the imino-chitosan biopolymer FTIR spectra can be observed in 3700–2700 cm^{-1} spectral region, where strong overlapping bands are assigned to different —OH stretching vibrations corresponding to intra- and inter-molecular H-bonds (Fig. 1b) (Marin et al., 2014). First, a new band located at higher wavenumber appeared (3409, 3436, 3447 cm^{-1}) suggesting the formation of new inter-molecular H-bonds (Sun et al., 2008). Second, the bands located around 3348 and 3256 cm^{-1} in chitosan FTIR spectrum are slightly shifted to higher wavenumbers (around 3370 cm^{-1}) and decrease in intensity in the imino-chitosan FTIR spectra – indicating weaker, rare intra-molecular H-bonds. Third, changes in terms of shape, band intensity and band frequency are observed in the 1500–1200 cm^{-1} spectral region, indicating changes in the environment of CH_2OH groups (Fig. 2s).

All above described spectral changes suggest a redistribution of the H-bonds, the inter-molecular ones becoming predominant as compared to the intra-molecular ones. The rational explanation is given by the imino-chitosan bonds formation which forces chitosan chains to straighten.

3.1. Morphology of the imino-chitosan biopolymeric films

The reversible nature of the imino covalent linkage under various conditions allows the aldehyde subcomponents to be displaced (Chen et al., 2013; Kovaříček & Lehn, 2012; Nasr et al., 2009) and therefore the self-assembling within supramolecular architectures to be kinetically controlled. Thus, the grafting of imine units as rigid side chains on the chitosan backbones must produce significant morphology changes which can be evidenced by wide angle X-ray diffraction.

Wide angle X-ray diffraction (WXRD) measurements were performed on imino-chitosan biopolymers and chitosan pellet

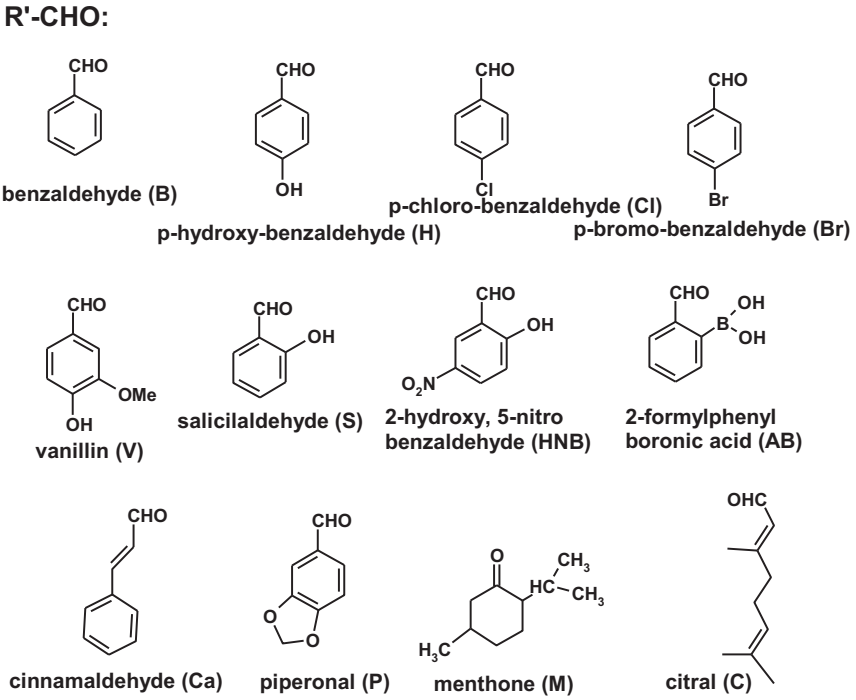

Scheme 1. Structure of the aldehydes used for biopolymer preparation.

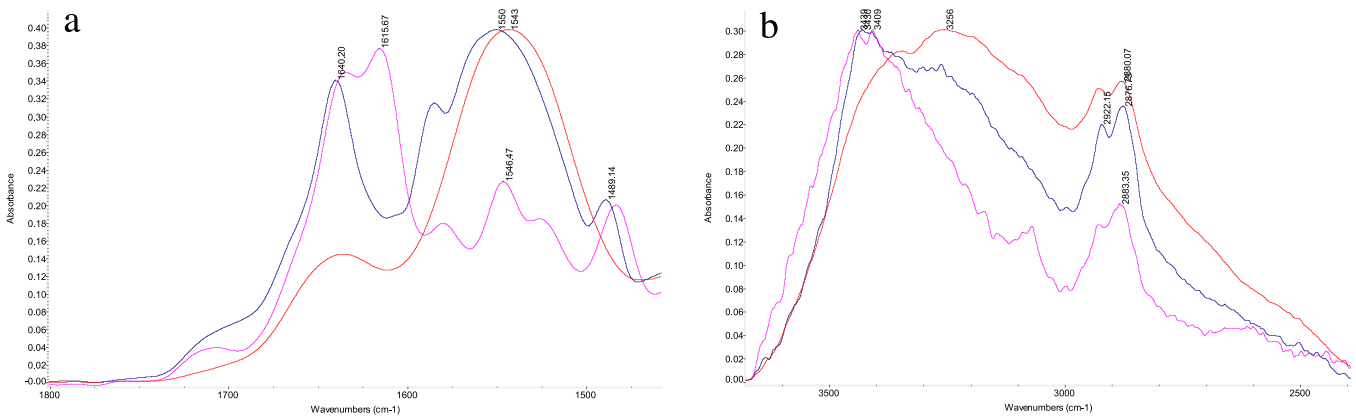

Fig. 1. FTIR spectra (ATR method) of chitosan (red), CHNB (violet) and CBr (blue) biopolymer films. (For interpretation of the references to color in figure legend, the reader is referred to the web version of the article.)

samples. Some representative WXRD diffractograms are given as an example in Fig. 2.

Chitosan X-ray diffraction profile exhibits a left tailed broad band located between 7 and 35°, with a maximum around 21° and a shoulder around 12°, indicating two overlapped reflections, characteristic to the crystallized phase form II (Leceta, Guerrero, Ibarburu, Duenas, & De la Caba, 2013). All the imino-chitosan samples exhibit, in the medium angle domain, a sharper band between 4.7 and 8.7°, a weak diffuse peak or shoulder with the intensity maximum around 11–15°, and a high intensity band with the maximum around 20°. This XRD pattern is characteristic to semicrystalline polyazomethines with thermotropic behavior (Marin, Perju, & Damaceanu, 2011; Zabulica, Perju, Bruma, & Marin, 2014). The d-spacing calculated with Bragg's law by using the measured diffraction angle is given in Table 1s. The three diffraction peaks and the corresponding d-spacing values suggest a supramolecular layered structure, rationally explained as the result of three ordering forces – hydrophobic/hydrophilic self-assembling, intermolecular H-bonding between chitosan chains, and aromatic–aromatic interactions.

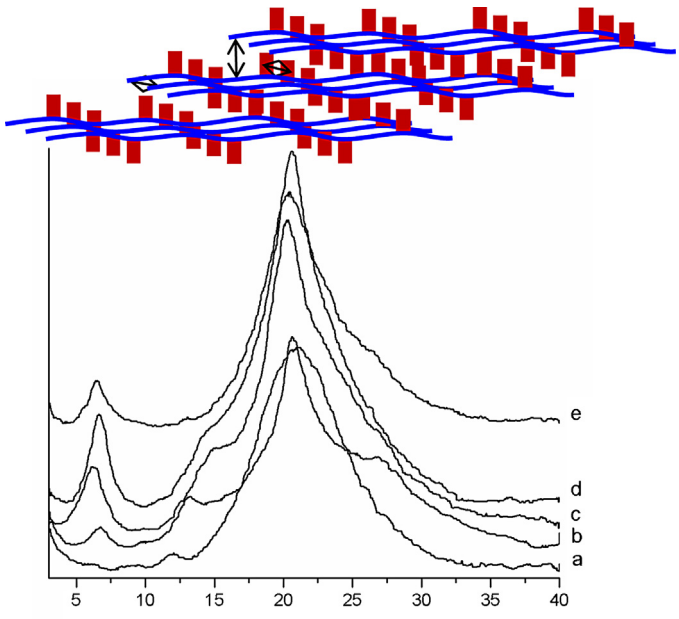

Fig. 2. XRD pattern of (a) chitosan, and (b) CHNB (c) CAB, (d) CS and (e) CH biopolymers.

Thus, the reflection at smaller angle characteristic for layering appears mainly due to the antagonistic character of the two components linked by imine linkage – the hydrophilic chitosan and the hydrophobic aldehyde – which tend to self-assemble in a similar manner as smectic mesophases of side chain liquid crystalline polymers (Baron, 2001). The narrow band reflects a quite exact interlayer distance value, indicating a quite uniform distribution of the imine units on chitosan chains. The trans-imination type exchange process plays an important role to an optimum arrangement of the imine units which further allows the stabilization of the layer structure through intermolecular H-bonds between chitosan backbones, H-bonds replacing the intramolecular ones with reaction progress. The inter-layer distance value ranges between 9.6 Å for benzaldehyde to 17.6 Å for cinnamaldehyde, in agreement with the different lengths of the obtained rigid imine units. The simulation of the molecular models by molecular mechanics MM+ method suggests an interdigitated motif (Baron, 2001) of the rigid newly formed imine core (Fig. 2). The band is sharper when aldehydes are more soluble in water (especially those containing hydroxyl group: vanillin, p-hydroxi benzaldehyde, o-hydroxi benzaldehyde, 2-formylphenyl boronic acid, 2-hydroxi, 5-nitro benzaldehyde, cinnamaldehyde) and more diffuse for the less soluble ones (p-chlor-benzaldehyde, p-brom-benzaldehyde, citral, menthone, piperonal), meaning that aldehyde solubility facilitates the layering.

The wide angle reflection of the imino-chitosan biopolymers is slightly shifted to higher d-spacing values (20°) as compared to chitosan (21°), revealing the new preponderant intermolecular distances which appear between two neighbor rigid imine units within a layer. The intermolecular distance corresponding to the intensity maximum is around 4.4 Å, indicating slight cohesive interactions between the rigid units.

The middle angle diffraction peak corresponds to the interchain distance between chitosan backbones. The weak diffuse peak is probably due to the different conformations adopted by imine units inside the layers, which determine a polydispersity of the distances between chitosan chains held together by weak intermolecular H-bonds (see FTIR study).

Therefore, WXRD diffractograms of the chitosan Schiff base biopolymers indicate a three dimensional architecture. Taking into consideration all above arguments brought by FTIR and WXRD measurements, a scenario of biopolymer forming can be drawn.

In solution, chitosan macromolecular chains are random coils, these facilitating strong intra-molecular H-bonds. Once the amine functional groups start to react with aldehyde reagents, the chitosan chains are forced to depart due to the newly formed bulky, rigid imine units, and thus the intramolecular H-bonds

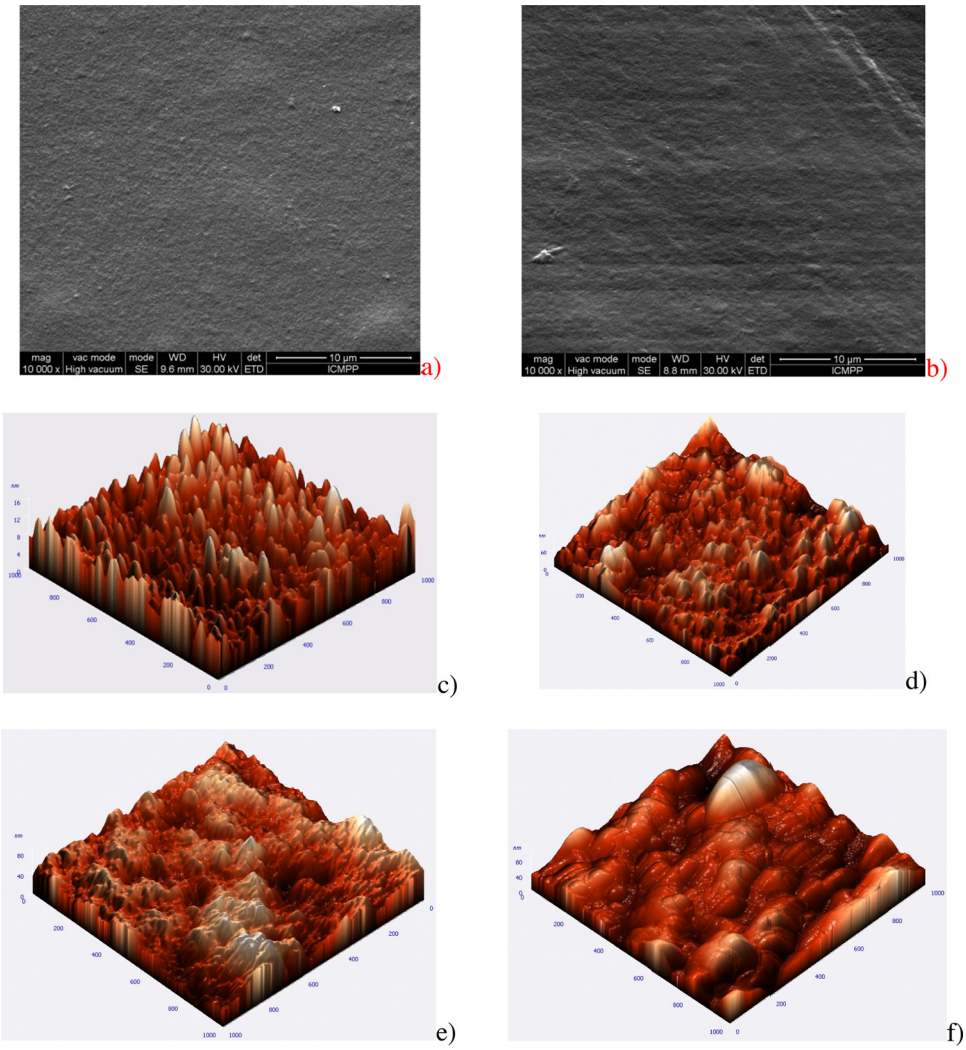

Fig. 3. Surface topography of (a) CH and (b) CBr biopolymers, as seen by SEM (10,000×); and (c) chitosan and (d) CC, (e) CH, (f) CC biopolymers as seen by AFM (1 μm × 1 μm).

slowly disappear and the free OH groups form new interchain H-bonds. With reaction progress, chitosan chains are forced to adopt a straight conformation, which facilitates the layering due to the hydrophilic/hydrophobic assembling of the chitosan/aromatic units. The reversibility of the covalent imine bond allows rearrangements of the rigid imine units by trans-imination reactions to reach a more compact, interdigitated motif. The reversible covalent bond formation and trans-imination process leads to dynamic covalent motion, driving self-assembling into a tri-dimensional architecture.

3.2. Film surface topography

The morphological changes into chitosan Schiff base biopolymers should be also reflected by film surface topography. To monitor them, SEM and AFM topographic and phase contrast measurements were performed on self-standing flexible films. SEM microphotographs show smooth film surfaces for all studied biopolymers (Fig. 3). A deeper view of film surface morphology was gain by AFM topographic images when a granular morphology was observed for all investigated biopolymers. The grain diameters range in the 40–200 nm domain, indicating a nanostructured surface (Table 2s). Some representative SEM and AFM images are given in Fig. 3.

All films have small values of the phase contrast shift of the contrast phase images (Table 2s), this indicating relief differences but not chemical composition variation and confirming once more the absence of unreacted aldehyde.

3.3. Dynamic mechanical analysis

To gain more information on the molecular motion of the imino-chitosan chains into the films, dynamic mechanical analysis (DMA) has been performed into the −150 to 350 °C temperature range. DMA studies on chitosan revealed a strong influence of hydrogen bonding physical network structure and water content on the viscoelastic behavior, mirrored by the γ-relaxation (Mano, 2008; Ogura, Kanamoto, Itoh, Miyashiro, & Tanaka, 1980).

Fig. 4a displays the variation of the storage modulus (E') and loss factor ($\tan\delta$) with temperature for some representative imino-chitosan biopolymers and the chitosan parent. As a general observation, γ and β_d relaxations appear for all samples, therefore residual water is present in the films but not in an amount that would vanish the γ-relaxation. Information on relaxations is summarized in Table 3s.

In the glassy region the storage modulus increases for the imino-chitosan biopolymers relative to the storage modulus of chitosan, indicating an increased rigidity, most probably due to a tridimensional biopolymer ordering. When the temperature exceeds −50 °C, the decrease of E' modulus as a result of the enhancement of residual water mobility is immediately followed by water removal. The

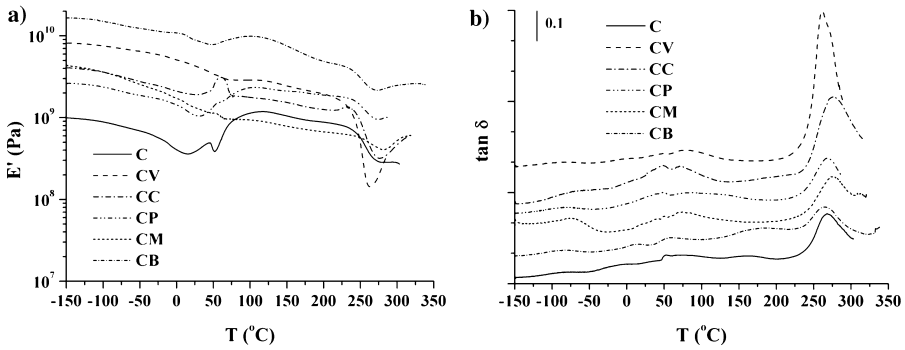

Fig. 4. (a) Variation of the storage modulus (E') with temperature (2 °C/min, 1 Hz); (b) variation of the loss factor (tan δ) with temperature (2 °C/min, 1 Hz) (the tan δ curves are represented relative to the same scale, but they are shifted for clarity).

effect is an instant upturn of E' modulus for C, CC, CP, CB samples, while a plateau appears for CV and CM samples. The rise of E' intensity normally depends on the content of residual water of the chitosan-based films. A change in the order of E' modulus value is observed after water release, i.e. chitosan becomes stiffer than CM, and CP becomes stiffer than CM and CC samples. This aspect can be explained based on the structures of the aldehyde fragment and the supramolecular assembling of the newly formed imino-chitosan derivatives. Menthone has not an aromatic ring, therefore the assembling into a π–π stacking structure is excluded, but menthone component could act as a plasticizer. The chitosan loses the plasticizing water and, in the absence of any plasticizer, its rigidity increases. A different situation is met in the case of piperonal – after water removal, the intramolecular π–π interaction between the aromatic rings intensifies and the E' modulus rises over the ones of CM and CC.

Thus, the DMA study proves that small amounts of residual water remain into the biopolymer structure even after in vacuum drying, facilitating the trans-imination processes and consequently the ordering processes even in the dry films.

3.4. Contact angle measurements and surface free energy calculation

The biomaterial surface is the first part coming into contact with cells or biological fluids. Thus, biocompatibility will be primarily influenced by the surface characteristics of the biomaterial, particularly the wettability, surface chemistry, surface energy and topography. Blood-contacting devices and tissue engineering substrates need an appropriate balance of hydrophilic/hydrophobic surface entities, excessive hydrophobic surfaces enhancing cell affinity and reducing biocompatibility, while highly hydrophilic surfaces prevent cell–cell interactions, particularly important in tissue engineering (Menzies & Jones, 2010).

To have a first insight on the potential biocompatibility of the studied biomaterials, their contact angle and surface free energy (SFE) were measured and the results are given in Fig. 5 and Table 1. As can be seen in Fig. 5, the studied biopolymer surface has a lower water-to-air contact angle value in comparison with the chitosan parent, this indicating an increased wettability. Except the menthone containing biopolymer, all the others show water-in-air contact angles in the range of 60–90° – characteristic to moderate wettable surfaces and most favorable for cell adhesion (Ikada, 1994). It can be appreciated that modification of chitosan by grafting various imine units on its backbone led to biopolymers more polar than chitosan, with more hydrophilic surfaces, with contact angle values within the moderate hydrophilicity range. The effect is more significant when chitosan is modified with (a) oxygen containing aldehydes (CH; CP) – which promote the wettability by H-bonding, or (b) aromatic aldehydes (CB, CCa) – which promote a good conjugation and thus polar structures. On the other hand, imino-chitosan biopolymers prepared from aliphatic aldehydes (CC, CM) or from the ones containing aliphatic units (CV) gave higher contact angle values (93°, 82°, 74°) indicating less hydrophilic surfaces, but still more hydrophilic as compared to parent chitosan.

Surface free energy (SFE) is a biomaterial characteristic which affects cellular adhesion, spreading and their migration – essential features in maintaining multicellular structure. It was demonstrated that biomaterials with high SFE value and polarity frequently exhibit high potential for cell culture applications (Hallab, Bundy, O'Connor, Moses, & Jacobs, 2001). The surface energy values obtained for parent and Schiff base modified chitosan samples are given in Table 1.

The total surface free energy (γ_s^{TOT}) of 29.53 mN/m experimentally calculated for the chitosan film sample can be regarded as a low energy surface, with a dominant dispersive Lifshitz–van der Waals contribution (γ_S^{LW}) and a low electron donating contribution (γ_S^-).

As compared to the parent chitosan, all studied biopolymers reveal higher γ_s^{TOT} values, suggesting that grafting of imine units on chitosan enhance the surface free energy. Moreover, both the dispersive (γ_S^{LW}) and polar (γ^{ab}) component values are also higher, which is logic considering the physical interactions occurring due to the electron rich imine units formation.

The higher hydrophilicity and thus wettability of the obtained biopolymers as compared to chitosan can be mainly explained by the intrinsic contribution of the new imine units and also by the layered morphology of the new biopolymer. The intrinsic contribution of the imine units can be divided into the intrinsic contributions of the polar imine linkages and on the other hand

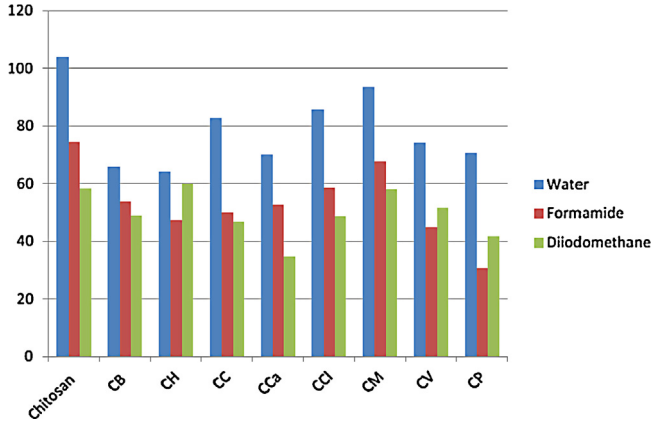

Fig. 5. Mean static contact angle between imino-chitosan film surfaces and water, formamide and diiodomethane.

Table 1
Surface free energy values and components for chitosan-modified surfaces in mN/m.

Samples	γ_S^{LW}	γ_S^+	γ_S^-	γ^{ab}	γ_s^{TOT}
Chitosan	29.51	0.19	6.57E−04	0.02	29.53
CB	34.86	0.21	18.29	3.88	38.74
CH	28.58	2.26	15.24	11.74	40.32
CC	36.05	1.72	1.58	3.29	39.35
CCa	42.12	0.01	12.56	0.84	42.97
CCl	35.03	0.59	2.29	2.34	37.38
CM	29.62	0.49	1.12	1.48	31.11
CV	33.31	2.61	5.06	7.27	40.58
CP	38.65	3.83	3.56	7.39	46.05

of the polar or non-polar aldehyde residues. An important contribution to the increased wettability is expected to be gained from the hydrophilic/hydrophobic self-assembling into a supramolecular structure. The layering (evidenced by WXRD) emancipates the hydroxyl groups from the intra-molecular H-bonding network and turn them in weak inter-molecular H-bonding (FTIR measurements), thus making them more available for new H-bonding links.

To conclude, the grafting of imine units on chitosan is a valid alternative to confer moderate hydrophilicity to biomaterials, making them promising candidates as scaffolds in tissue engineering.

3.5. Antimicrobial activity

To avoid the influence of acetic acid or unreacted aldehydes, the antimicrobial activity of the studied biopolymers has been assayed on the dried films. Three different reference strains – *E. coli* ATCC 25922, *S. aureus* ATCC 6583 and *C. albicans* ATCC 10231 – which are common and virulent pathogen agents met in care-associated diseases have been considered.

The antimicrobial activity was measured by the agar disk diffusion method which supposes the addition of the biopolymer film on the culture medium pre-inoculated with the microbial suspension, and measuring of the clear zone caused by growth inhibition around the film disks after 24 h of incubation. Some data on the average inhibition diameters and images of the inhibition zones of imino-chitosan films are given in Fig. 6.

First, one can observe that all films killed the bacterial culture placed in direct contact and almost all the studied biopolymers also inhibited the microbial growth on a large area around the film.

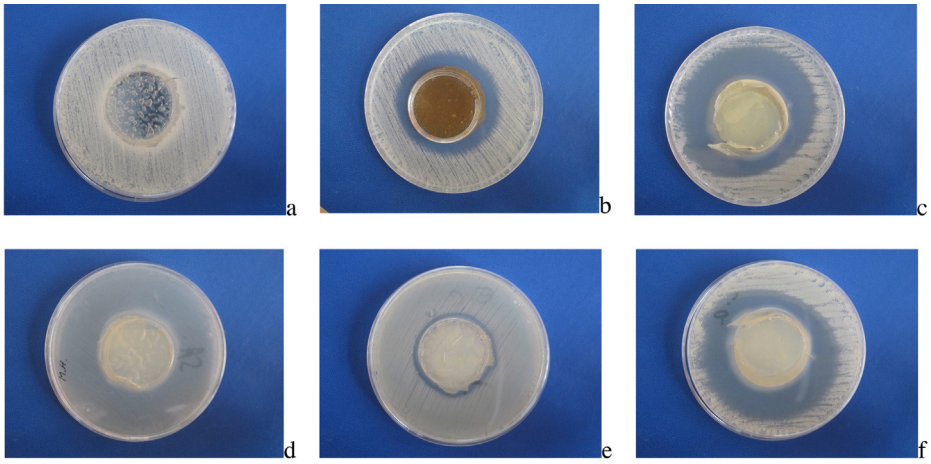

Antifungal activity of a) chitosan, b) CP , c) CAB against *C. albicans* yeast and antimicrobial activity of CCl biopolymer against d) *S. aureus*, e) *E. coli*, f) *C. albicans*

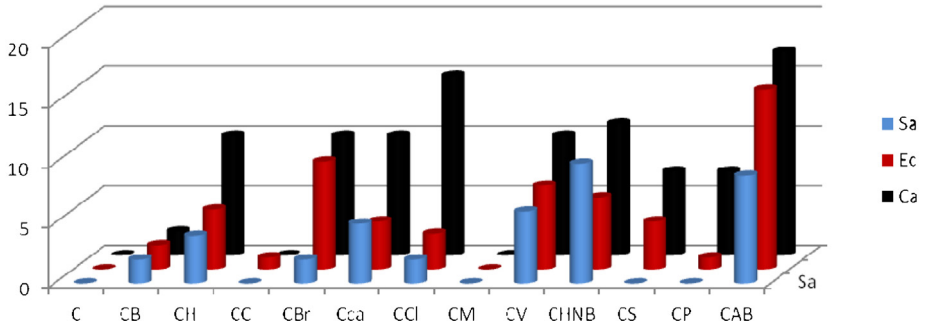

Fig. 6. Inhibition zone (mm) of the imino-chitosan biopolymers.

The chitosan control films did not show any inhibition zone for the tested bacterial strains. The biopolymers obtained from hydroxyl containing aldehydes present the highest activity against gram positive bacteria (e.g. *S. aureus*). According to literature data, HO— containing compounds can bond to lipoteichoic acid on cell surface and disrupt membrane functions (Raafat et al., 2008). The low activity of the 2-hydroxy-benzaldehyde (salycilaldehyde) containing biopolymers can be explained by the strong H-bonding of the ortho-OH to the electron pair of imine nitrogen, which hinders imine reversibility. On the other hand, the biopolymer obtained from the 2-hydroxy-5-nitro-benzaldehyde exhibits the most intense activity against the gram positive *S. aureus* – activity which can be assigned to the influence of the nitro group (Nada et al., 2014).

As concerns the activity of the studied biopolymers against gram negative bacteria (e.g. *E. coli*), it appears that the best activity has been obtained for the biopolymer based on the boric acid containing aldehyde (CAB). This high activity can be attributed to the electron deficient boron atom, which competes with stabilizing divalent metals (e.g. Mg^{2+}, Ca^{2+}) in the cell wall, leading to structural destabilization (Raafat et al., 2008). This mechanism applies well to the other biopolymers with good *E. Coli* inhibition activity; the strong electron donating groups (—Br, —OH) promote good electron delocalization by conjugation with electron withdrawing imine unit, and consequently the appearance of electron deficient sites.

Except the biopolymers obtained from benzaldehyde or aliphatic/cycloaliphatic aldehydes, all other biopolymer films show very good inhibition activity against *C. albicans* yeast. In fact, these biopolymers (CB, CC, CM) also showed the lowest activity against Gram (+) and Gram (−) bacteria, this underlining the importance of functional groups upon fungicidal and antibacterial activity.

An interesting observation comes from the biopolymer obtained from cinnamaldehyde, that shows a fairly good activity against all studied microorganisms. However, the best activity was revealed by the biopolymer containing boric acid. The results suggest further investigations, taking into account that both biopolymers can form hydrogels (Marin et al., 2012, 2014) which can be applied as scaffolds for bone or skin regeneration.

4. Conclusions

Twelve imino-chitosan biodinameric films have been prepared to investigate the effect of imine bonds reversibility on film preparation and properties. FTIR spectra and WXRD diffractograms proved the structuring of the biopolymer in a three-dimensional morphology formed by alternating hydrophilic chitosan and hydrophobic imine unit layers. The three-dimensional architecture is facilitated by the good aldehyde solubility in water, which ensures enough time for imine links reassembling through forming and trans-imination processes. Moreover, small amounts of residual water remain into biopolymer structure even after drying, facilitating the trans-imination processes and consequently ordering processes even in the dry films. The alternating hydrophilic/hydrofobic layers ensure a good balance of hydrophilic/hydrophobic surface entities and yield a moderate wettability – a first feature of a biocompatible material. Moreover, the imino-chitosan films have a smooth, nanostructured surface which favors cellular adhesion and proliferation. Furthermore, the imino-chitosan films show self-defence properties; they inhibit bacteria and strain growth on large areas surrounding the film, and appear to be potential materials able to prevent biofilm formation – i.e. of potential interest as integrated parts of the organism. The imine reversibility assures a slow release of the antimicrobial aldehyde in microbiological environment, the reaction equilibrium moving once the aldehyde is consumed.

This study proves that imine units grafted on chitosan chains assisted by dynamic covalent chemistry offer interesting opportunities to obtain valuable biomaterials with highly controlled structures and morphologies.

Acknowledgements

This work was financially supported by the Romanian National Authority for Scientific Research, CNCS – UEFISCDI grant, project number PN-II-ID-PCCE-2011-2-0028 and European Union's Seventh Framework Program (FP7/2007–2013) under grant agreement no. 264115 – STREAM.

Appendix A. Supplementary data

Supplementary data associated with this article can be found, in the online version, at http://dx.doi.org/10.1016/j.carbpol.2014.10.050.

References

An, J., Ji, Z., Wang, D. S., Luo, Q., & Li, X. (2014). Preparation and characterization of uniform-sized chitosan/silver microspheres with antibacterial activities. *Materials Science & Engineering C: Materials for Biological Applications*, *36*, 33–41.

Baron, M. (2001). Definitions of basic terms relating to low-molar-mass and polymer liquid crystals. *Pure and Applied Chemistry*, *73*, 845–895.

Brugnerotto, J., Lizardi, J., Goycoolea, F. M., Arguelles-Monal, W., Desbrieres, J., & Rinaudo, M. (2001). An infrared investigation in relation with chitin and chitosan characterization. *Polymer*, *42*, 3569–3580.

Cado, G., Aslam, R., Seon, L., Garnier, T., Fabre, R., Parat, A., et al. (2013). Self-defensive biomaterial coating against bacteria and yeasts: Polysaccharide multilayer film with embedded antimicrobial peptide. *Advanced Functional Materials*, *23*, 4801–4809.

Caro, C. A., Cabello, G., Landaeta, E., Perez, J., Zagal, J. H., & Lillo, L. (2013). Synthesis and spectroscopic and electrochemical studies of chitosan Schiff base derivatives. *Russian Journal of Applied Chemistry*, *86*, 1791–1797.

Chen, L., Chen, Z., Li, X., Huang, W., Li, X., & Liu, X. (2013). Dynamic imine chemistry assisted reaction induced hetero-epitaxial crystallization: Novel approach towards aromatic polymer/CNT nanohybrid shish-kebabs and related hybrid crystalline structures. *Polymer*, *54*, 1739–1745.

Croisier, F., & Jérôme, C. (2013). Chitosan-based biomaterials for tissue engineering. *European Polymer Journal*, *49*, 780–792.

Ferrero, F., Periolatto, M., Vineis, C., & Varesano, A. (2014). Chitosan coated cotton gauze for antibacterial water filtration. *Carbohydrate Polymers*, *103*, 207–212.

Guinesi, L. S., & Cavalheiro, E. T. G. (2006). Influence of some reactional parameters on the substitution degree of biopolymeric Schiff bases prepared from chitosan and salicylaldehyde. *Carbohydrate Polymers*, *65*, 557–561.

Guo, Z. Y., Ren, J. M., Dong, F., Wang, G., & Li, P. C. (2013). Comparative study of the influence of active groups of chitosan derivatives on antifungal activity. *Journal of Applied Polymer Science*, *127*, 2553–2556.

Hallab, N., Bundy, K., O'Connor, K., Moses, R. L., & Jacobs, J. J. (2001). Evaluation of metallic and polymeric biomaterial surface energy and surface roughness characteristics for directed cell adhesion. *Tissue Engineering*, *7*, 55–71.

Ikada, Y. (1994). Surface modification of polymers for medical applications. *Biomaterials*, *15*, 726–736.

Kim, K. W., Min, B. J., Kim, Y. T., Kimmel, R. M., Cooksey, K., & Park, S. I. (2011). Antimicrobial activity against foodborne pathogens of chitosan biopolymer films of different molecular weights. *LWT – Food Science and Technology*, *44*, 565–569.

Kovaříček, P., & Lehn, J.-M. (2012). Merging constitutional and motional covalent dynamics in reversible imine formation and exchange processes. *Journal of the American Chemistry Society*, *134*, 9446–9455.

Kumar, S., Kumari, M., Dutta, P. K., & Koh, J. (2014). Chitosan biopolymer Schiff base: Preparation, characterization, optical, and antibacterial activity. *International Journal of Polymeric Materials and Polymeric Biomaterials*, *63*, 173–177.

Leceta, I., Guerrero, P., Ibarburu, I., Duenas, M. T., & De la Caba, K. (2013). Characterization and antimicrobial analysis of chitosan-based films. *Journal of Food Engineering*, *116*, 889–899.

Mano, J. (2008). Viscoelastic properties of chitosan with different hydration degrees as studied by dynamic mechanical analysis. *Macromolecular Bioscience*, *8*, 69–76.

Marin, L., Perju, E., & Damaceanu, D. (2011). Designing thermotropic liquid crystalline polyazomethines based on fluorene and/or oxadiazole chromophores. *European Polymer Journal*, *47*, 1284–1299.

Marin, L., Simionescu, B. C., & Barboiu, M. (2012). Imino-chitosan biodynamers. *Chemical Communications*, *48*, 8778–8780.

Marin, L., Harabagiu, V., van der Lee, A., Arvinte, A., & Barboiu, M. (2013). Structure-directed functional properties of symmetrical and unsymmetrical Br-substituted Schiff-bases. *Journal of Molecular Structure*, *1049*, 377–385.

Marin, L., Popescu, M.-C., Zabulica, A., Uji, H., I, & Fron, E. (2013). Chitosan as matrix for bio-polymer dispersed liquid crystal systems. *Carbohydrate Polymers*, *95*, 16–24.

Marin, L., Stoica, I., Mares, M., Dinu, V., Simionescu, B. C., & Barboiu, M. (2013). Antifungal vanillin–imino-chitosan biodynameric films. *Journal of Materials Chemistry B*, *1*, 3353–3358.

Marin, L., Moraru, S., Popescu, M.-C., Nicolescu, A., Zgardan, C., Simionescu, B. C., et al. (2014). Out-of-water constitutional self-organization of chitosan–cinnamaldehyde dynagels. *Chemistry: A European Journal*, *20*, 4814–4821.

Menzies, K. L., & Jones, L. (2010). The impact of contact angle on the biocompatibility of biomaterials. *Optometry & Vision Science*, *87*, 387–399.

Muzzarelli, R. A. A. (2009). Genipin-chitosan hydrogels as biomedical and pharmaceutical aids. *Carbohydrate Polymers*, *77*, 1–9.

Muzzarelli, R. A. A., & Muzzarelli, C. (2009). Chitin and chitosan hydrogels. In G. O. Phillips, & P. A. Williams (Eds.), *Handbook of hydrocolloids* (2nd ed., pp. 849–888). Cambridge, UK: Woodhead Publishing Ltd.

Muzzarelli, R. A. A., Tanfani, F., Emanuelli, M., & Mariotti, S. (1982). N-Carboxymethylidene chitosans and N-carboxymethyl chitosans: Novel chelating polyampholytes obtained from chitosans glyoxylate. *Carbohydrate Research*, *107*, 199–219.

Muzzarelli, R. A. A., Ilari, P., Xia, W., Pinotti, M., & Tomasetti, M. (1994). Tyrosinase-mediated quinone tanning of chitinous materials. *Carbohydrate Polymers*, *24*, 294–300.

Muzzarelli, R. A. A., Littarru, G. P., Muzzarelli, C., & Tosi, G. (2003). Selective reactivity of biochemically relevant quinones towards chitosans. *Carbohydrate Polymers*, *53*, 109–115.

Nada, A. A., James, R., Shelke, N. B., Harmon, M. D., Awad, H. M., Nagarale, R. K., et al. (2014). A smart methodology to fabricate electrospun chitosan nanofiber matrices for regenerative engineering applications. *Polymers for Advanced Technologies*, *25*, 507–515.

Nasr, G., Petit, E., Vullo, D., Wilnum, J.-Y., Supuran, C. T., & Barboiu, M. (2009). Carbonic anhydrase-encoded dynamic constitutional libraries: Toward the discovery of isozyme-specific inhibitors. *Journal of Medicinal Chemistry*, *52*, 4853–5359.

Ogura, K., Kanamoto, T., Itoh, M., Miyashiro, H., & Tanaka, H. (1980). Dynamic mechanical behavior of chitin and chitosan. *Polymer Bulletin*, *2*, 301–304.

Park, S., Ahn, S. H., Lee, H. J., Chung, U. S., Kim, J. H., & Koh, W. G. (2013). Mesoporous TiO_2 as a nanostructured substrate for cell culture and cell patterning. *RSC Advances*, *3*, 23673–23680.

Peng, Y., & Li, Y. (2014). Combined effects of two kinds of essential oils on physical, mechanical and structural properties of chitosan films. *Food Hydrocolloid*, *36*, 287–293.

Raafat, D., von Bargen, K., Haas, A., & Sahl, H. G. (2008). Insights into the mode of action of chitosan as an antibacterial compound. *Applied and Environmental Microbiology*, *74*, 3764–3773.

Ravi Kumar, M. N. V., Muzzarelli, R. A. A., Muzzarelli, C., Sashiwa, H., & Domb, A. J. (2004). Chitosan chemistry and pharmaceutical perspectives. *Chemical Reviews*, *104*, 6017–6084.

Sagiomo, V., & Luning, U. (2009). On the formation of imines in water – a comparison. *Tetrahedron Letters*, *50*, 4663–4665.

Saito, Y., Luchnikov, V., Inaba, A., & Tamura, K. (2014). Self-scrolling ability of differentially acetylated chitosan film. *Carbohydrate Polymers*, *109*, 44–48.

Sanjai, C., Kothan, S., Gonil, P., Saesoo, S., & Sajomsang, W. (2014). Chitosan-triphosphate nanoparticles for encapsulation of super-paramagnetic iron oxide as an MRI contrast agent. *Carbohydrate Polymers*, *104*, 231–237.

Sun, Y., Lin, L., Deng, H., Li, J., He, B., Sun, R., et al. (2008). Structural changes of bamboo cellulose in formic acid. *BioResources*, *3*, 297–315.

van Oss, C. J., Chaudhury, M. K., & Good, R. J. (1988). Interfacial Lifshitz-van der Waals and polar interactions in macroscopic systems. *Chemical Reviews*, *88*, 927–941.

Vasile, C., & Pascu, M. C. (2007). *Surfaces properties of polymers*. Trivandrum, India: Research Signpost.

Yudin, V. E., Dobrovolskaya, I. P., Neelov, I. M., Dresvyanina, E. N., Popryadukhin, P. V., Ivankova, E. M., et al. (2014). Wet spinning of fibers made of chitosan and chitin nanofibrils. *Carbohydrate Polymers*, *108*, 176–182.

Zabulica, A., Perju, E., Bruma, M., & Marin, L. (2014). Novel luminescent liquid crystalline polyazomethines. Synthesis and study of thermotropic and photoluminescent properties. *Liquid Crystal*, *41*, 252–262.